We are IntechOpen, the world's leading publisher of Open Access books Built by scientists, for scientists

4,800
Open access books available

122,000
International authors and editors

135M
Downloads

Our authors are among the

154
Countries delivered to

TOP 1%
most cited scientists

12.2%
Contributors from top 500 universities

CLARIVATE ANALYTICS BOOK CITATION INDEX INDEXED

WEB OF SCIENCE™

Selection of our books indexed in the Book Citation Index in Web of Science™ Core Collection (BKCI)

Interested in publishing with us?
Contact book.department@intechopen.com

Numbers displayed above are based on latest data collected.
For more information visit www.intechopen.com

Chapter 6

Static, Vibration, and Buckling Analysis of Nanobeams

Şeref Doğuşcan Akbaş

Additional information is available at the end of the chapter

http://dx.doi.org/10.5772/67973

Abstract

Static, vibration, and buckling analysis of nanobeams is studied based on modified couple stress theory (MCST) in this chapter. The inclusion of an additional material parameter enables the new beam model to capture the size effect. The new nonclassical beam model reduces the classical beam model when the length scale parameter is set to zero. The finite element formulations are derived for static, free vibration, and buckling problems of nanobeams within MCST and the Euler-Bernoulli beam theory. The effect of the material length scale parameter and geometry parameters on the static, vibration, and buckling responses of the nanobeam is investigated in both the classical beam theory (CBT) and MCST by using finite element method. Also, the difference between the classical beam theory (CBT) and modified couple stress theory is investigated.

Keywords: nanobeams, couple stress theory, finite element method, static, vibration, buckling

1. Introduction

With the great advances in technology in recent years, micro and nanostructures have found many applications. In these structures, micro beams and micro tubes are widely used in nanoscale electromechanical systems such as sensors (Zook et al. [1], Pei et al. [2]), actuators (Senturia [3], Rezazadeh et al. [4]). In investigation of micro and nanostructures, the classical continuum mechanics are not effort of describing of the size-dependent mechanics. Nonclassical continuum theories such as higher-order gradient theories and the couple stress theory are capable of explanation of the size-dependent behaviors, which occur in micro/nanoscale structures.

At the present time, the experimental investigations of the micro/nano materials are still a challenge because of difficulties confronted in the micro/nanoscale. Therefore, mechanical

theories and atomistic simulations have been used for nanostructural analysis. The process of the atomistic simulations is very difficult and takes much time. So, continuum theory is the most preferred method for the analysis of the micro and nanostructures. Classical continuum mechanics does not contain the size effect, because of its scale-free character. The nonlocal continuum theory initiated by Eringen [5] has been widely used to mechanical behavior of micro/nanostructures.

The size effect is very effective in the mechanical behavior of nanostructures at nanometer scale that the classic theory has failed to consider when the size reduces from macro to nano (Toupin [6], Mindlin [7, 8], Fleck and Hutchinson [9], Yang et al. [10], Lam et al. [11]). Therefore, higher-order theories of modified couple stress theory (MCST) and modified strain gradient are used in the mechanical model of the nano/microstructures (Yang et al. [10], Lam et al. [11]).

The determination of the micro/nanostructural material length scale parameters is very difficult experimentally. So, Yang et al. [10] studied the strain energy of the MCST with one length scale parameter. After this, the MCST and the strain gradient elasticity theories have been widely applied to static and dynamic analysis of beams (Park and Gao [12], Ma et al. [13], Kong et al. [14], Wang et. al. [15], Asghari et al. [16], Wang [17], Simsek [18], Kahrobaiyan et al. [19], Xia et al. [20], Ke et al. [21], Li et al. [22], Akgöz and Civalek [23, 24], Ansari et al. [25], Dos Santos and Reddy [26], Simsek et al. [27], Wang et al. [28], Kocatürk and Akbas [29], Kong [30], Daneshmehr et al. [31], Akgöz and Civalek [32], Ziaee [33], Islam et. al. [34], Miandoab et al. [35], Liu et al. [36], Tang et al. [37], Hosseini and Rahmani [38], Akbas [39, 40]).

The objective of this paper is to investigate static, vibration, and buckling solutions of nanobeams based on modified couple stress theory (MCST). The finite element formulations are derived for static, free vibration, and buckling problems of nanobeams within MCST and the Euler-Bernoulli beam theory. The effect of the material length scale parameter and geometry parameters on the static, vibration, and buckling responses of the nanobeam are investigated in both the classical beam theory (CBT) and MCST. Also, the difference between the classical beam theory and modified couple stress theory is investigated.

2. Theory and formulations

A simple supported nanobeam of length *L*, width *b*, and height *h*, with *X,Y,Z* cartesian coordinate system is shown in **Figure 1**.

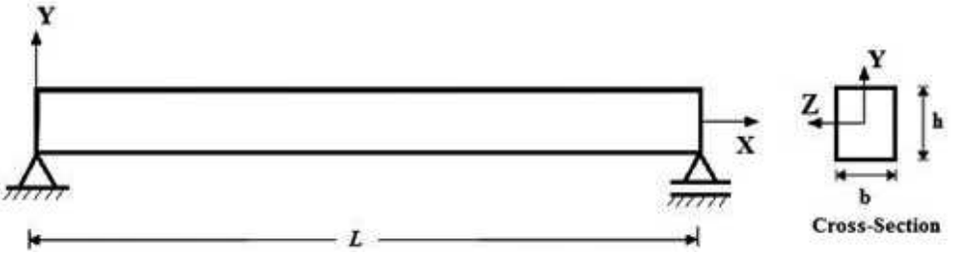

Figure 1. A simple supported nanobeam with *X,Y,Z* cartesian coordinate system and cross section.

http://dx.doi.org/10.5772/67973

The modified couple stress theory was proposed by Yang et al. [10]. Based on this theory, the strain energy density for a linear elastic material which is a function of both strain tensor and curvature tensor is introduced for the modified couple stress theory;

$$U = \int_V (\boldsymbol{\sigma} : \boldsymbol{\varepsilon} + \boldsymbol{m} : \boldsymbol{\chi})\, dV \tag{1}$$

where $\boldsymbol{\sigma}$ is the stress tensor, $\boldsymbol{\varepsilon}$ is the strain tensor, $\boldsymbol{m}$ is the deviatoric part of the couple stress tensor, $\boldsymbol{\chi}$ is the symmetric curvature tensor, defined by

$$\boldsymbol{\sigma} = \lambda\ tr(\boldsymbol{\varepsilon}) I + 2\mu\boldsymbol{\varepsilon} \tag{2}$$

$$\boldsymbol{\varepsilon} = \frac{1}{2}[\nabla \boldsymbol{u} + (\nabla \boldsymbol{u})^T] \tag{3}$$

$$\boldsymbol{m} = 2l^2 \mu\, \boldsymbol{\chi} \tag{4}$$

$$\boldsymbol{\chi} = \frac{1}{2}[\nabla \boldsymbol{\theta} + (\nabla \boldsymbol{\theta})^T] \tag{5}$$

where λ and μ are Lame's constants, l is a material length scale parameter which is regarded as a material property characterizing the effect of couple stress, $\boldsymbol{u}$ is the displacement vector and $\boldsymbol{\theta}$ is the rotation vector, given by

$$\boldsymbol{\theta} = \frac{1}{2}\text{curl}\ \boldsymbol{u} \tag{6}$$

The parameters λ and μ in the constitutive equation are given by

$$\lambda = \frac{E\,\nu}{(1+\nu)(1-2\nu)},\ \mu = \frac{E}{2(1+\nu)} \tag{7}$$

where E is the modulus of elasticity and ν is the Poisson's ratio. According to the coordinate system *(X,Y,Z)* shown in **Figure 1**, based on Euler-Bernoulli beam theory, the axial and the transverse displacement field are expressed as

$$u(X, Y, t) = u_0(X, t) - Y\frac{\partial v_0(X, t)}{\partial X} \tag{8}$$

$$v(X, Y, t) = v_0(X, t) \tag{9}$$

$$w(X, Y, t) = 0 \tag{10}$$

where u, v, w are the x, y, and z components of the displacements, respectively; u_0 and v_0 are the axial and the transverse displacements in the mid-plane; and t indicates time. Because the transversal surfaces of the beam are free of stress,

$$\sigma_{zz} = \sigma_{yy} = 0 \tag{11}$$

By using Eqs. (3) and (8)–(10), the strain-displacement relation can be obtained:

$$\varepsilon_{xx} = \frac{\partial u}{\partial X} = \frac{\partial u_0(X,t)}{\partial X} - Y\frac{\partial^2 v_0(X,t)}{\partial X^2} \tag{12a}$$

$$\varepsilon_{yy} = \varepsilon_{zz} = Y\frac{\nu\,\partial^2 v_0(X,t)}{\partial X^2} \tag{12b}$$

$$\varepsilon_{xz} = \varepsilon_{yz} = \varepsilon_{xy} = 0 \tag{12c}$$

By using Eqs. (6) and (8)–(10),

$$\theta_z = \frac{\partial v_0(X,t)}{\partial X}\theta_x = \theta_y = 0 \tag{13}$$

Substituting Eq. (13) into Eq. (5), the curvature tensor χ can be obtained as follows:

$$\chi_{xz} = \frac{1}{2}\frac{\partial^2 v_0(X,t)}{\partial X^2}\chi_{xx} = \chi_{xy} = \chi_{yy} = \chi_{yz} = \chi_{zz} = 0 \tag{14}$$

According to Hooke's law, the constitutive equations of the nanobeam are as follows:

$$\sigma_{xx} = E\varepsilon_{xx} = E\left[\frac{\partial u_0(X,t)}{\partial X} - Y\frac{\partial^2 v_0(X,t)}{\partial X^2}\right] \tag{15}$$

where σ_{xx} and ε_{xx} are the normal stresses and normal strains in the X direction, respectively. Substituting Eq. (14) into Eq. (4), the couple stress tensor can be obtained as follows:

$$m_{xz} = l^2\mu\frac{1}{2}\frac{\partial^2 v_0(X,t)}{\partial X^2} \tag{16a}$$

$$m_{xx} = m_{xy} = m_{yy} = m_{yz} = m_{zz} = 0 \tag{16b}$$

where μ is the shear modulus defined by Eq. (7). The elastic strain energy (Ui) of the nanobeam is expressed as

$$U_i = \frac{1}{2}\int_0^L\int_A(\sigma_{ij}\ \varepsilon_{ij} + m_{ij}\ \chi_{ij})dA\ dX \tag{17}$$

By substituting Eqs. (12) and (14)–(16) into Eq. (17), elastic strain energy (U_i) can be rewritten as follows:

$$U_i = \frac{1}{2}\int_0^L\left[EA\left(\frac{\partial u_0(X,t)}{\partial X}\right)^2 + EI\left(\frac{\partial^2 v(X,t)}{\partial X^2}\right)^2 + \frac{1}{4}l^2\mu A\left(\frac{\partial^2 v(X,t)}{\partial X^2}\right)^2\right]dX \tag{18}$$

where A is the area of the cross section, and I is the moment of inertia.

http://dx.doi.org/10.5772/67973

$$T = \frac{1}{2}\int_0^L \left[\rho A\left(\frac{\partial u_0}{\partial t}\right)^2 + \rho A\left(\frac{\partial v_0}{\partial t}\right)^2 + \rho I\left(\frac{\partial^2 v_0}{\partial X\,\partial t}\right)^2\right] dX \tag{19}$$

The potential energy of the external load can be written as

$$U_e = \int_0^L \left[f\ v(x) + P\left(\frac{\partial v}{\partial x}\right)\right] dX + Q_i v_i \tag{20}$$

where f is load function, Q_i is point loads which contains point forces and moments, P is axial compressive load for buckling case. The nodal displacements q for a two-node beam element contain three degrees of freedom at each node, as shown in **Figure 2**, namely,

$$\{q(t)\}_{\mathrm{e}} = [u_i^{(e)}(t),\ v_i^{(e)}(t),\ \ \theta_i^{(e)}(t),\ u_j^{(e)}(t),\ v_j^{(e)}(t),\ \ \theta_j^{(e)}(t)\ ]^T \tag{21}$$

The displacement field of the finite element is expressed in terms of the nodal displacements as follows:

$$u^{(\mathrm{e})}(X,\mathrm{t}) = \varphi_1^{(U)}(X)\ u_{\mathrm{i}}(t) + \varphi_2^{(U)}(X)\ u_{\mathrm{j}}(t)\ = [\varphi^{(U)}]\begin{Bmatrix} u_{\mathrm{i}} \\ u_{\mathrm{j}} \end{Bmatrix} = [\varphi^{(U)}]\{\mathrm{q}\}_U \tag{22}$$

$$v^{(\mathrm{e})}(X,\mathrm{t}) = \varphi_1^{(V)}(X)\ v_{\mathrm{i}}(t) + \varphi_2^{(V)}(X)\ \theta_{\mathrm{i}}(t) + \varphi_3^{(V)}(X)\ v_{\mathrm{j}}(t) + \varphi_4^{(V)}(X)\ \theta_{\mathrm{j}}(t) \tag{23a}$$

$$\left[\varphi^{(V)}\right]\begin{Bmatrix} v_{\mathrm{i}} \\ \theta_{\mathrm{i}} \\ v_{\mathrm{j}} \\ \theta_{\mathrm{j}} \end{Bmatrix} = \left[\varphi^{(V)}\right]\{q\}_V \tag{23b}$$

where u_{i}, v_{i}, and θ_{i} are the axial displacements, transverse displacements, and slopes at the two end nodes of the beam element, respectively, and $\varphi_{\mathrm{i}}^{(U)}$ and $\varphi_{\mathrm{i}}^{(V)}$ are the Hermite shape functions for the axial and transverse displacements, respectively. The interpolation functions for the axial displacement are,

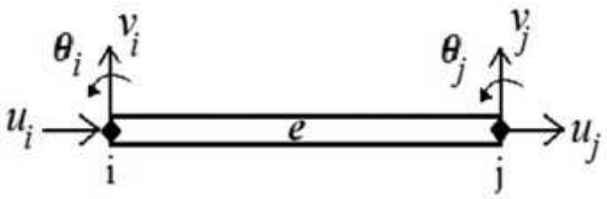

Figure 2. Two-node beam element.

$$\varphi^{(U)}(\mathrm{X}) = \left[\varphi_1^{(U)}(\mathrm{X})\ \varphi_2^{(U)}(\mathrm{X})\right]^T \tag{24}$$

where

$$\varphi_1^{(U)}(\mathrm{X}) = \left(-\frac{X}{L_\mathrm{e}} + 1\right) \tag{25a}$$

$$\varphi_2^{(U)}(\mathrm{X}) = \left(\frac{X}{L_\mathrm{e}}\right) \tag{25b}$$

The interpolation functions for the transverse displacement are

$$\varphi^{(V)}(\mathrm{X}) = \left[\varphi_1^{(V)}(\mathrm{X})\ \varphi_2^{(V)}(\mathrm{X})\ \varphi_3^{(V)}(\mathrm{X})\ \varphi_4^{(V)}(\mathrm{X})\right]^T \tag{26}$$

where

$$\varphi_1^{(V)}(\mathrm{X}) = \left(1 - \frac{3X^2}{L_\mathrm{e}^2} + \frac{2X^3}{L_\mathrm{e}^3}\right) \tag{27a}$$

$$\varphi_2^{(V)}(\mathrm{X}) = \left(-X + \frac{2X^2}{L_\mathrm{e}} - \frac{X^3}{L_\mathrm{e}^2}\right) \tag{27b}$$

$$\varphi_3^{(V)}(\mathrm{X}) = \left(\frac{3X^2}{L_\mathrm{e}^2} - \frac{2X^3}{L_\mathrm{e}^3}\right) \tag{27c}$$

$$\varphi_4^{(V)}(\mathrm{X}) = \left(\frac{X^2}{L_\mathrm{e}} - \frac{X^3}{L_\mathrm{e}^2}\right) \tag{27d}$$

with L_e indicating the length of the beam element. The Lagrangian functional of the problem is given as follows:

$$I = T - (U_\mathrm{i} + U_\mathrm{e}) \tag{28}$$

After substituting Eqs. (22) and (23) into Eq. (28) and then using the Lagrange's equations, one obtains the following equation:

$$\frac{\partial I}{\partial q_k^{(e)}} - \frac{\partial}{\partial t}\frac{\partial I}{\partial \dot{q}_k^{(e)}} = 0, k = 1, 2, 3, 4, 5, 6, \tag{29}$$

where $\dot{q}_k^{(e)}$ indicates the time derivative of the nodal displacements q.

The Lagrange's equations can be employed to yield the system of equations of motion for the finite element. By the usual assemblage procedure, the equations of motion can be obtained for the entire structure. For the free vibration problem, the finite element equation is as follows:

http://dx.doi.org/10.5772/67973

$$([K] - \omega^2[M])\{\hat{q}\} = 0 \tag{30}$$

For the static problem, the finite element equation is as follows:

$$[K]\{q\} = \{F\} \tag{31}$$

For the buckling problem, the finite element equation is as follows:

$$([K] - P_{cr}[K_G])\{\hat{q}\} = 0 \tag{32}$$

where ω is the natural frequency, $\{\hat{q}\}$ is a vector of displacement amplitudes of the vibration, $\{F\}$ is the global load vector, $[K]$ is the stiffness matrix, $[M]$ is the mass matrix, and $[K_G]$ is the stability matrix. The stiffness matrix $[K]$ can be given as:

$$[K] = \begin{bmatrix} [K^A] & [0] \\ [0] & [K^D] \end{bmatrix} \tag{33}$$

where

$$[K^A] = \int_0^{L_e} EA \left[\frac{\partial \varphi^{(U)}}{\partial X}\right]^T \left[\frac{\partial \varphi^{(U)}}{\partial X}\right] dX \tag{34a}$$

$$[K^D] = \int_0^{L_e} \left(\mathrm{EI} + \frac{1}{4} l^2 \mu A\right) \left[\frac{\partial^2 \varphi^{(V)}}{\partial X^2}\right]^T \left[\frac{\partial^2 \varphi^{(V)}}{\partial X^2}\right] dX \tag{34b}$$

The mass matrix $[M]$ can be expressed as the sum of four submatrices as follows:

$$[M] = [M_U] + [M_V] + [M_\varnothing] \tag{35}$$

where

$$[M_U] = \int_0^{L_e} \rho A [\varphi^{(U)}]^T [\varphi^{(U)}] dX \tag{36a}$$

$$[M_V] = \int_0^{L_e} \rho A [\varphi^{(V)}]^T [\varphi^{(V)}] dX \tag{36b}$$

$$[M_\varnothing] = \int_0^{L_e} \rho I [\varphi^{(\varnothing)}]^T [\varphi^{(\varnothing)}] dX \tag{36c}$$

The stability matrix $[K_G]$ can be given as:

$$[K_G] = \begin{bmatrix} [0] & [0] \\ [0] & [K_G^D] \end{bmatrix} \tag{37}$$

where

$$[K_G^D] = \int_0^{L_e} \left[\frac{\partial \varphi^{(V)}}{\partial X}\right]^T \left[\frac{\partial \varphi^{(V)}}{\partial X}\right] dX \tag{38}$$

The load vector $\{F\}$ is expressed as

$$\{F\} = \int_{x=0}^{L_e} \{\varphi(X)\}^T f \, dX + Q_i \tag{39}$$

In the solution of the free vibration and buckling problems, the eigenvalue procedure is performed in Eqs. (30) and (32). When the material length scale parameter (l) is equal to zero, the finite element formulations reduce to classical beam theory.

After integration processing, the finite element matrixes can be expressed as follows:

$$[K] = \begin{bmatrix} \frac{EA}{L_e} & 0 & 0 & -\frac{EA}{L_e} & 0 & 0 \\ 0 & \frac{12(EI+0.25l^2\mu A)}{{L_e}^3} & \frac{-6(EI+0.25l^2\mu A)}{{L_e}^2} & 0 & \frac{-12(EI+0.25l^2\mu A)}{{L_e}^3} & \frac{-6(EI+0.25l^2\mu A)}{{L_e}^2} \\ 0 & \frac{-6(EI+0.25l^2\mu A)}{{L_e}^2} & \frac{4(EI+0.25l^2\mu A)}{L_e} & 0 & \frac{6(EI+0.25l^2\mu A)}{{L_e}^2} & \frac{2(EI+0.25l^2\mu A)}{L_e} \\ -\frac{EA}{L_e} & 0 & 0 & \frac{EA}{L_e} & 0 & 0 \\ 0 & \frac{-12(EI+0.25l^2\mu A)}{{L_e}^3} & \frac{6(EI+0.25l^2\mu A)}{{L_e}^2} & 0 & \frac{12(EI+0.25l^2\mu A)}{{L_e}^3} & \frac{6(EI+0.25l^2\mu A)}{{L_e}^2} \\ 0 & \frac{-6(EI+0.25l^2\mu A)}{{L_e}^2} & \frac{2(EI+0.25l^2\mu A)}{L_e} & 0 & \frac{6(EI+0.25l^2\mu A)}{{L_e}^2} & \frac{4(EI+0.25l^2\mu A)}{L_e} \end{bmatrix} \tag{40a}$$

$$[M] = \begin{bmatrix} \frac{\rho AL_e}{3} & 0 & 0 & \frac{\rho AL_e}{6} & 0 & 0 \\ 0 & (\frac{13\rho AL_e}{35} + \frac{6\rho I}{5L_e}) & (\frac{-11\rho A{L_e}^2}{210} - \frac{\rho I}{10}) & 0 & (\frac{9\rho AL_e}{70} - \frac{6\rho I}{5L_e}) & (\frac{13\rho A{L_e}^2}{420} - \frac{\rho I}{10}) \\ 0 & (\frac{-11\rho A{L_e}^2}{210} - \frac{\rho I}{10}) & (\frac{\rho A{L_e}^3}{105} + \frac{2\rho IL_e}{15}) & 0 & (\frac{-13\rho A{L_e}^2}{420} + \frac{\rho I}{10}) & \frac{-\rho A{L_e}^3}{140} - \frac{\rho IL_e}{30} \\ \frac{\rho AL_e}{6} & 0 & 0 & \frac{\rho AL_e}{3} & 0 & 0 \\ 0 & (\frac{9\rho AL_e}{70} - \frac{6\rho I}{5L_e}) & (\frac{-13\rho A{L_e}^2}{420} + \frac{\rho I}{10}) & 0 & (\frac{13\rho AL_e}{35} + \frac{6\rho I}{5L_e}) & (\frac{11\rho A{L_e}^2}{210} + \frac{\rho I}{10}) \\ 0 & (\frac{13\rho A{L_e}^2}{420} - \frac{\rho I}{10}) & (\frac{-\rho A{L_e}^3}{140} - \frac{\rho IL_e}{30}) & 0 & (\frac{11\rho A{L_e}^2}{210} + \frac{\rho I}{10}) & (\frac{\rho A{L_e}^3}{105} + \frac{2\rho IL_e}{15}) \end{bmatrix} \tag{40b}$$

http://dx.doi.org/10.5772/67973

$$[K_G] = \begin{bmatrix} 0 & 0 & 0 & 0 & 0 & 0 \\ 0 & \frac{6}{5L_e} & \frac{-1}{10} & 0 & \frac{-6}{5L_e} & \frac{-1}{10} \\ 0 & \frac{-1}{10} & \frac{2L_e}{15} & 0 & \frac{1}{10} & \frac{-L_e}{30} \\ 0 & 0 & 0 & 0 & 0 & 0 \\ 0 & \frac{-6}{5L_e} & \frac{1}{10} & 0 & \frac{6}{5L_e} & \frac{1}{10} \\ 0 & \frac{-1}{10} & \frac{-L_e}{30} & 0 & \frac{1}{10} & \frac{2L_e}{15} \end{bmatrix} \tag{40c}$$

3. Numerical results

In the numerical examples, the effects of the material length scale parameter and geometry parameters on the static, vibration, and buckling responses of the nanobeam are presented in both the classical beam theory (CBT) and MCST. Using the conventional assembly procedure for the finite elements, the system stiffness, mass, stability matrices, and the load vector are obtained from the element stiffness, mass, stability matrices, and load vectors. After that, the solution process outlined in the preceding section is used to obtain the solution for the problem of concern. In obtaining the numerical results, graphs and solution of the nonlinear finite element model, MATLAB program is used. The nanobeam is taken to be made of epoxy ($E = 1{,}44$ GPa, $\nu = 0.38$, $l = 17.6$ μm, $\rho = 1600\,\frac{\text{kg}}{\text{m}^3}$). In the numerical calculations, the number of finite elements is taken as 100. In the numerical integrations, five-point Gauss integration rule is used.

In order to establish the accuracy of the present formulation and the computer program developed by the author, the results obtained from the present study are compared with the available results in the literature. For this purpose, the static deflections shapes of a simple supported beam with rectangular cross section, which is subjected to a point load, are calculated for MCST and compared with those of Alashti and Abolghasemi [41] by inserting the material and load properties used in this reference. It is clearly seen that the curves of **Figure 3** of the present study are very close to those of Alashti and Abolghasemi [41].

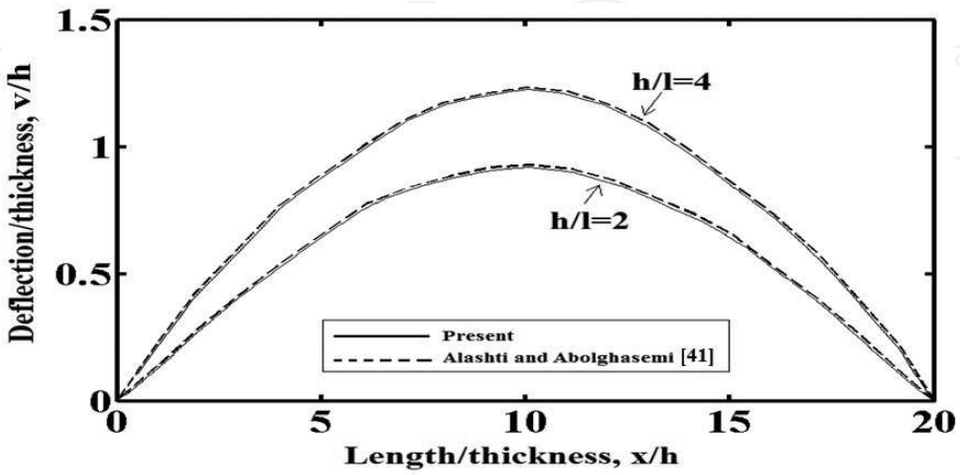

Figure 3. Comparison study: static deflections shape of the simple supported beam based on the MCST.

Figure 4a–c shows the effects of the thickness (h) on the static, vibration, and buckling responses of the nanobeam, respectively, in both the CBT and MCST. In these figures, static deflections, fundamental frequencies, and critical buckling loads are calculated and plotted for different values of the h for $b = l$ and $L = 30\ l$. In the calculation of **Figure 3a**, the nanobeam is subjected to a transversal point load ($P = 100\ \mu N$) at the midpoint of the beam in the transverse direction.

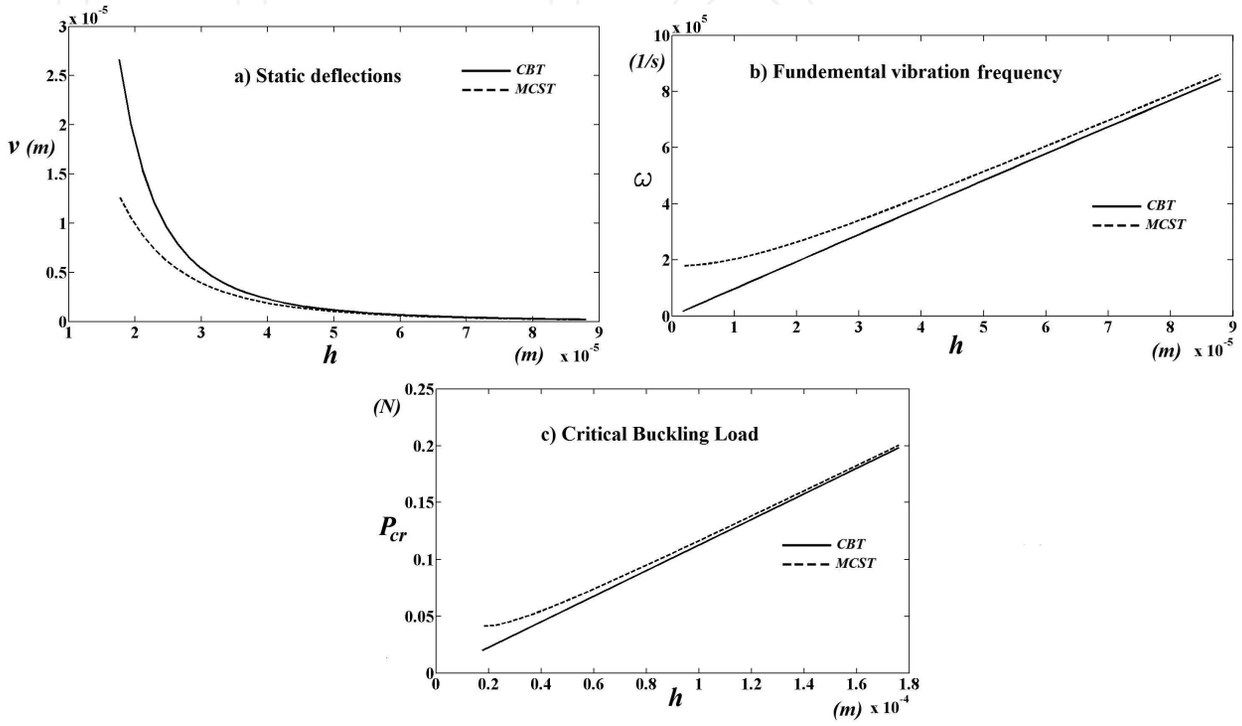

Figure 4. Effect of the thickness on the static, vibration, and buckling responses of the nanobeam for CBT and MCST; (a) static analysis, (b) free vibration analysis, and (c) buckling analysis.

As seen from **Figure 4**, the difference between the results of the MCST and CBT decreases significantly with the increase in the thickness of the nanobeam. Increase in the thickness of the nanobeam leads to a decline on effects of size effect and difference between the results of MCST and CBT.

In order to see the effect of material length scale parameter (l) on the static, vibration and buckling of the nanobeam, static deflections, fundamental frequencies, and critical buckling loads are displayed with different value of the dimensionless material length scale parameters (l/h) in both the CBT and MCST in **Figure 5** for $b = 1\ \mu m$ and $L = 30\ \mu m$. In this figure, for different values of the dimensionless material length scale parameters (l/h), the material length scale parameter (l) is varied when the thickness of the nanobeam (h) is kept constant as $1\ \mu m$.

It is seen from **Figure 5** that with an increase in the dimensionless material length scale parameter l/h leads to a rise on the difference between the results of the MCST and CBT. Also, the dimensionless material length scale parameter has no effect on the mechanical responses for the classical theory, which is unable to capture the size effect. It is found that the deflections

http://dx.doi.org/10.5772/67973

of the nanobeam by the CBT are always larger than those by the MCST. However, fundamental frequencies and critical buckling loads by the MCST are always larger than those by the CBT. It can be seen from figures that the difference between the CBT and MCST is very large when the h and l/h increase. The material parameter and dimension of the nanobeam have a very important role on the mechanical behavior of nanobeams.

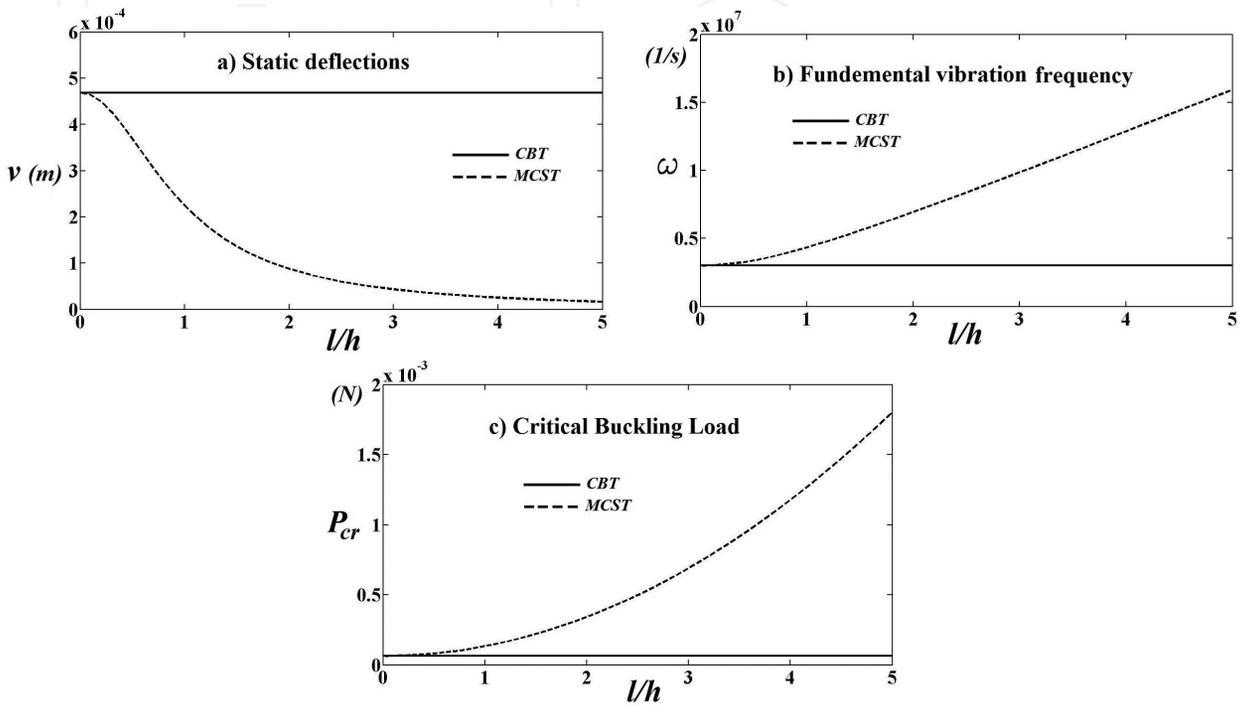

Figure 5. Effect of the dimensionless material length scale parameter (l/h) on the static, vibration, and buckling responses of the nanobeam for CBT and MCST; (a) static analysis, (b) free vibration analysis, and (c) buckling analysis.

4. Conclusions

Finite element solution of nanobeams is investigated based on modified couple stress theory within the Euler-Bernoulli beam theory. The finite element formulations are derived for static, free vibration, and buckling problems of nanobeams. The effect of the material length scale parameter and geometry parameters on the static, vibration, and buckling responses of the nanobeam is presented and discussed in the numerical study. Also, the difference between the classical beam theory and modified couple stress theory is investigated.

It is observed from the investigations that the material length scale parameter and dimension of the nanobeam have a big influence on the static, free vibration, and buckling behaviors of nanobeams. With the increase in the thickness of the nanobeam (h) and decrease in the dimensionless material length scale parameter (l/h), the difference between the classical beam theory and modified couple stress theory decrease considerably. It is observed from the results that modified couple stress theory must be used instead of the classical beam theory for small values of nanobeam height and high values of the material length scale parameter.

Author details

Şeref Doğuşcan Akbaş

Address all correspondence to: serefda@yahoo.com

Department of Civil Engineering, Bursa Technical University, Bursa, Turkey

References

[1] Zook J.D., Burns D.W., Guckel H., Smegowsky J.J., Englestad R.L. and Feng Z. Characteristics of polysilicon resonant microbeams. Sensors and Actuators. 1992;**35**:31–59.

[2] Pei J., Tian F. and Thundat T. Glucose biosensor based on the microcantilever. Analytical Chemistry. 2004;**76**:292–297.

[3] Senturia S.D. CAD challenges for microsensors, microactuators, and microsystems. Proceeding of IEEE. 1998;**86**:1611–1626.

[4] Rezazadeh G., Tahmasebi A. and Zubtsov M. Application of piezoelectric layers in electrostatic MEM actuators: controlling of pull-in voltage. Journal of Microsystem Technologies. 2006;**12**:1163–1170.

[5] Eringen A.C. Nonlocal polar elastic continua. International Journal Engineering and Science. 1972;**10**(1):1–16.

[6] Toupin R.A. Elastic materials with couple stresses. Archive for Rational Mechanics and Analysis. 1962;**11**:385–414.

[7] Mindlin R.D. and Tiersten H.F. Effects of couple-stresses in linear elasticity. Archive for Rational Mechanics and Analysis. 1962;**11**:415–448.

[8] Mindlin R.D. Influence of couple-stresses on stress concentrations. Experimental Mechanics. 1963;**3**:1–7.

[9] Fleck H.A. and Hutchinson J.W. A phenomenological theory for strain gradient effects in plasticity. Journal of Mechanics and Physics of Solids. 1993;**41**:1825–57.

[10] Yang F. Chong A., Lam D. and Tong P. Couple stress based strain gradient theory for elasticity. International Journal of Solids and Structures. 2002;**39**(10):2731–2743.

[11] Lam D.C.C., Yang F., Chong A.C.M., Wang J. and Tong P. Experiments and theory in strain gradient elasticity. Journal of Mechanics and Physics of Solids. 2003;**51**(8):1477–508.

[12] Park S.K. and Gao X.L. Bernoulli–Euler beam model based on a modified couple stress theory. Journal of Micromechanics and Microengineering. 2006;**16**:2355–2359.

[13] Ma H.M., Gao X.L. and Reddy J.N. A microstructure-dependent Timoshenko beam model based on a modified couple stress theory. Journal of Mechanics and Physics of Solids. 2008;**56**:3379–3391.

[14] Kong S.L., Zhou S., Nie Z. and Wang K. The size-dependent natural frequency of Bernoulli–Euler micro-beams. International Journal of Engineering Science. 2008;**46**:427–437.

[15] Wang C.M., Xiang Y. and Kitipornchai S. Postbuckling of nano rods/tubes based on nonlocal beam theory. International Journal of Applied Mechanics. 2009;**1**(2):259–266.

[16] Asghari M., Ahmadian M.T., Kahrobaiyan M.H. and Rahaeifard M. On the size dependent behavior of functionally graded micro-beams. Materials Design. 2010;**31**:2324–3249.

[17] Wang L. Size-dependent vibration characteristics of fluid-conveying microtubes. Journal of Fluids and Structure. 2010;**26**:675–684.

[18] Simsek M. Dynamic analysis of an embedded microbeam carrying a moving microparticle based on the modified couple stress theory. International Journal of Engineering Science. 2010;**48**:1721–1732.

[19] Kahrobaiyan M.H., Asghari M., Rahaeifard M. and Ahmadian M.T. Investigation of the size dependent dynamic characteristics of atomic force microscope microcantilevers based on the modified couple stress theory. International Journal of Engineering Science. 2010;**48**:1985–1994.

[20] Xia W., Wang L. and Yin L. Nonlinear non-classical microscale beams: static, bending, postbuckling and free vibration. International Journal of Engineering Science. 2010;**48**:2044–2053.

[21] Ke L.L.,Wang Y.S. and Wang Z.D. Thermal effect on free vibration and buckling of size-dependent microbeams. Physica E: Low-Dimensional Systems and Nanostructures. 2011;**43**(7):1387–1393.

[22] Li, C., Lim C.W., Yu J.L. and Zeng Q.C. Analytical solutions for vibration of simply supported nonlocal nanobeams with an axial force. International Journal of Structural Stability and Dynamics. 2011;**11**:257–271.

[23] Akgöz B. and Civalek Ö. Analysis of microtubules based on strain gradient elasticity and modified couple stress theories. Advances in Vibration Engineering. 2012;**11**(4):385–400.

[24] Akgöz B. and Civalek Ö. Longitudinal vibration analysis for microbars based on strain gradient elasticity theory. Journal of Vibration and Control. 2012;**20**(4):606–616.

[25] Ansari R., Gholami R. and Darabi M.A. A nonlinear Timoshenko beam formulation based on strain gradient theory. Journal of Mechanics of Materials and Structures. 2012;**7**(2):95–211.

[26] Dos Santos J.A. and Reddy J.N. Free vibration and buckling analysis of beams with a modified couple-stress theory. International Journal of Applied Mechanics. 2012;**4** (3):1250026.

[27] Simsek M., Kocatürk T. and Akbas S.D. Static bending of a functionally graded microscale Timoshenko beam based on the modified couple stress theory. Composite Structures. 2013;**95**:740–747.

[28] Wang L., Xu Y.Y. and Ni Q. Size-dependent vibration analysis of three-dimensional cylindrical microbeams based on modified couple stress theory: a unified treatment. International Journal of Engineering Science. 2013;**68**:1–10.

[29] Kocatürk T. and Akbas S.D. Wave propagation in a microbeam based on the modified couple stress theory. Structural Engineering and Mechanics. 2013;**46**:417–431.

[30] Kong S.L. Size effect on natural frequency of cantilever micro-beams based on a modified couple stress theory. Advanced Materials Research. 2013;**694**:221–224.

[31] Daneshmehr A.R., Abadi M.M. and Rajabpoor A. Thermal effect on static bending, vibration and buckling of reddy beam based on modified couple stress theory. Applied Mechanics and Materials. 2013;**332**:331–338.

[32] Akgöz B. and Civalek Ö. Buckling analysis of linearly tapered micro-Columns based on strain gradient elasticity. Structural Engineering and Mechanics. 2013;**48**(2):195–205.

[33] Ziaee S. Buckling of defective carbon nanotubes under axial and transverse loads. International Journal of Applied Mechanics. 2014;**6**(1):1450004.

[34] Islam Z.M., Jia P. and Lim C.W. Torsional wave propagation and vibration of circular nanostructures based on nonlocal elasticity theory. International Journal of Applied Mechanics. 2014;**6**(2):1450011.

[35] Miandoab E.M., Pishkenari H.N. and Yousefi-Koma A. Dynamic analysis of electrostatically actuated nanobeam based on strain gradient theory. International Journal of Structural Stability and Dynamics. 2015;**15**(4):1450059.

[36] Liu C., Ke L., Yang Y., Yang J., and Kitipornchai S. Buckling and post-buckling of size-dependent piezoelectric timoshenko nanobeams subject to thermo-electro-mechanical loadings. International Journal of Structural Stability and Dynamics. 2013;**14**(4):1–22.

[37] Tang M., Ni Q., Wang L., Luo Y. and Wang Y. Size-dependent vibration analysis of a microbeam in flow based on modified couple stress theory. International Journal of Engineering Science. 2014;**85**:20–30.

[38] Hosseini S.A.H. and Rahmani O. Surface effects on buckling of double nanobeam system based on nonlocal Timoshenko model. International Journal of Structural Stability and Dynamics. 2016;**16**:1550077.

[39] Akbas S.D. Analytical solutions for static bending of edge cracked micro beams. Structural Engineering and Mechanics. 2016;**59**(3):579–599.

[40] Akbas S.D. Forced vibration analysis of viscoelastic nanobeams embedded in an elastic medium. Smart Sructures and Systems. 2016;**18**(6):1125–1143.

[41] Alashti R. A. and Abolghasemi A.H. A size-dependent Bernoulli-Euler beam formulation based on a new model of couple stress theory. International Journal of Engineering-Transactions C: Aspects. 2013; **27**(6):951–960.

IntechOpen

IntechOpen